

## Chapter 2

# T2K Experiment

The T2K experimental setup consists of the J-PARC accelerator, a neutrino beamline, near detectors and a far detector (Super-K) as illustrated in Fig. 2.1. The T2K neutrino beamline is configured such that the far detector is  $2.5^\circ$  off the beamline axis. Since it is an important feature of the T2K experiment, it is described in the beginning of this chapter (Sect. 2.1). Then, details of the hardware components (Sects. 2.2, 2.3, 2.4 and 2.5) and data set acquired until May 2013 (Sect. 2.6) are explained.

### 2.1 Off-Axis Beam Configuration

When a neutrino is produced from the pion two-body decay, the neutrino energy in the laboratory system ( $E_\nu$ ) is described as:

$$E_\nu = \frac{m_\pi^2 - m_\mu^2}{2(E_\pi - p_\pi \cos \theta_\nu)}, \quad (2.1)$$

where,  $m_\pi$  and  $m_\mu$  are the pion and muon masses,  $E_\pi$  and  $p_\pi$  are the pion energy and momentum and  $\theta_\nu$  is the angle between the pion and neutrino directions. Figure 2.2 shows the relation between  $p_\pi$  and  $E_\nu$  in the two body decay for some  $\theta_\nu$ . When  $\theta_\nu$  is shifted from zero, the energy of a neutrino from the two-body decay weakly depends on the pion momentum [1]. In T2K, the neutrino beam is purposely directed at  $2.5^\circ$  with respect to the baseline connecting the production target and Super-K as shown in Fig. 2.1. This feature makes the narrow-band neutrino beam toward Super-K. The  $2.5^\circ$  off-axis angle was determined so that the neutrino beam has a peak energy at  $\sim 0.6$  GeV, which maximizes the neutrino oscillation probabilities at 295 Km as shown in Fig. 2.3. In addition, it reduces background neutrino interactions; our signal is charged current quasi-elastic (CCQE) interaction as explained in Chap. 1 and the main background is charged current pion production ( $\text{CC}1\pi$ ) and neutral current pion

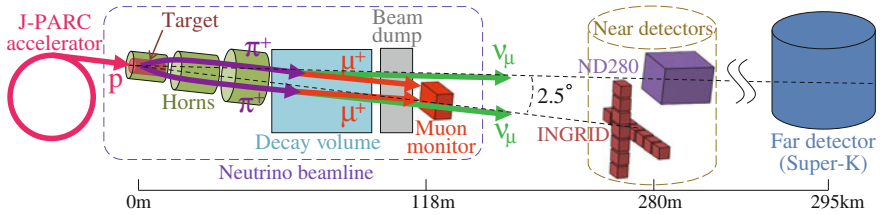
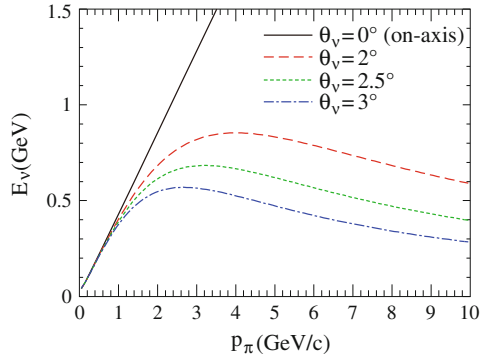


**Fig. 2.1** Schematic view of the T2K hardware components

**Fig. 2.2** The relation between pion momentum ( $p_\pi$ ) and neutrino energy ( $E_\nu$ ) in the pion two body decay



production ( $\text{NC}1\pi$ ) interaction. T2K is the first experiment that adopts the off-axis beam configuration.<sup>1</sup> However, the off-axis neutrino beam is very sensitive to the off-axis angle, hence a deviation of neutrino beam direction causes a large uncertainty of the neutrino beam. For example, when the neutrino beam direction deviates by 1 mrad, the intensity and peak energy of the neutrino beam at Super-K are predicted to change by 5 and 3 %, respectively. To achieve the target sensitivities in T2K, the neutrino beam direction is required to be controlled within 1 mrad and be measured with a much better precision.

## 2.2 J-PARC Accelerator

J-PARC [3] consists of three accelerators as shown in Fig. 2.4.

- A linear accelerator (LINAC) accelerates an  $\text{H}^-$  beam up to 400 MeV (181 MeV as of May 2013) and converts it to an  $\text{H}^+$  beam by charge-stripping foils.
- A rapid-cycling synchrotron (RCS) accelerates the beam up to 3 GeV with a 25 Hz cycle.

<sup>1</sup>The  $\text{NO}\nu\text{A}$  experiment [2] which started in 2014 also adopts the off-axis beam configuration.

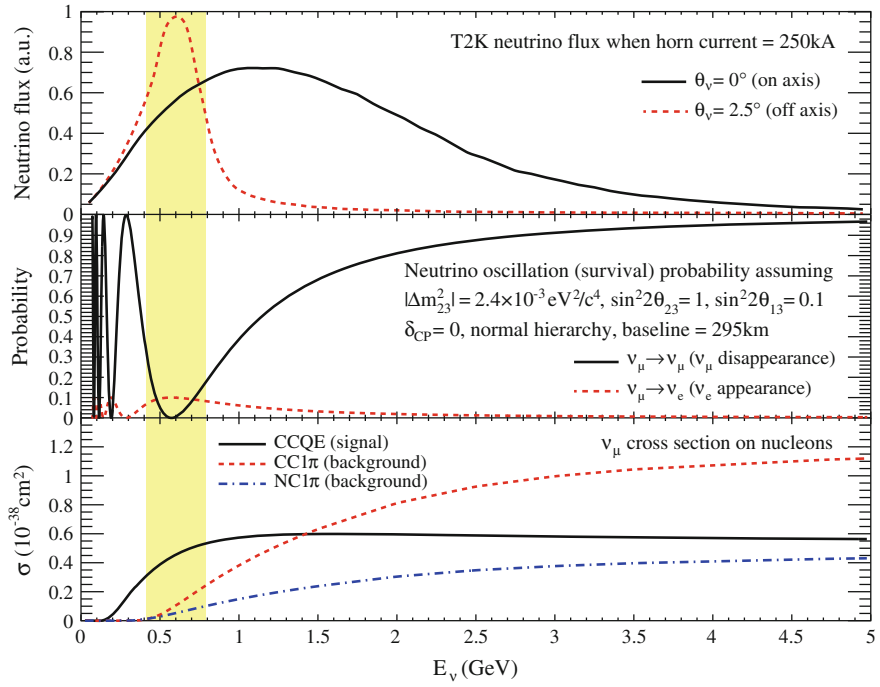


**Fig. 2.3** Neutrino energy spectra on axis and  $2.5^\circ$  off axis (*top*), neutrino oscillation (*survival*) probabilities (*middle*), and neutrino interaction cross sections divided by the neutrino energy (*bottom*) as a function of the neutrino energy

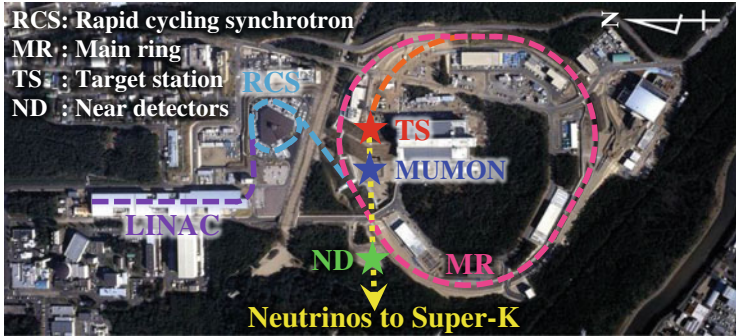


**Fig. 2.4** The J-PARC site viewed from above

- A main ring (MR) synchrotron takes about 5% of the beam<sup>2</sup> and accelerates it up to 30 GeV.

<sup>2</sup>The rest of the beam is supplied to the muon and neutron beamline in the Material and Life Science Facility (MLF).

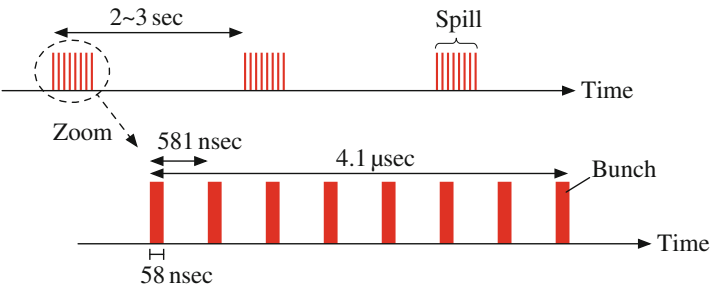


**Fig. 2.5** Schematic view of the beam spill

**Table 2.1** Design and present values of the fast extracted proton beam to the T2K neutrino beamline

Parameter	Design value	Present value (May, 2013)
Beam power	750 kW	220 kW
Beam kinetic energy	50 GeV	30 GeV
Number of protons	$3.3 \times 10^{14}$ /spill	$1.2 \times 10^{14}$ /spill
Number of bunches	8 bunches/spill	8 bunches/spill
Spill interval	3.3 s	2.48 s
Bunch interval	581 ns	581 ns
Bunch width	58 ns	58 ns
Spill width	4.1 μs	4.1 μs

For each acceleration cycle, the beam is fast-extracted from the MR to the T2K neutrino beamline as a “spill”. One spill contains eight bunches in  $4.1 \mu\text{s}$  as illustrated in Fig. 2.5. The design values of the extracted proton beam to the T2K neutrino beamline are listed in Table 2.1 together with the present values as of May 2013. J-PARC is designed to produce the most powerful beam (design intensity is 750 kW) in the world. This feature increases the intensity of the neutrino beam.

### 2.3 T2K Neutrino Beamline

The T2K neutrino beamline is composed of two sections: the primary and secondary beamlines. In the primary beamline, the extracted protons from MR are bent toward the direction of Super-K. In the secondary beamline, they collide with graphite target, producing secondary pions and other hadrons, which are focused by magnetic horns and decay into neutrinos. An overview of the neutrino beamline is illustrated in Fig. 2.6.

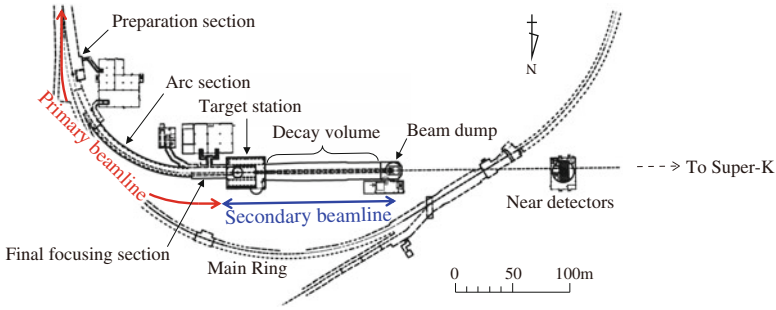


**Fig. 2.6** Overview of the T2K neutrino beamline

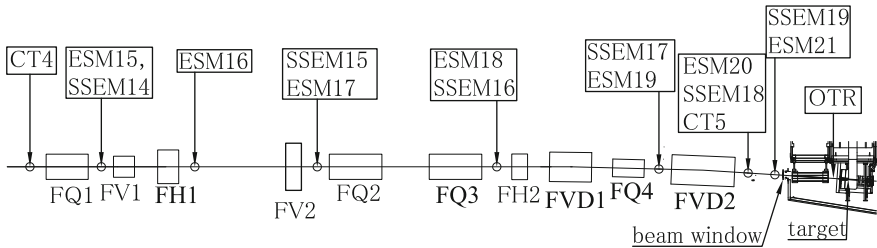


**Fig. 2.7** Location of the primary *beamline* monitors in the final focusing section

### 2.3.1 Primary Beamline

The primary beamline consists of the preparation ( $\sim 50$  m long), arc ( $\sim 150$  m) and final focusing ( $\sim 40$  m) sections as shown in Fig. 2.6. In the preparation section, the extracted proton beam is tuned with a series of 11 normal conducting magnets so that the beam can be accepted by the arc section. In the arc section, the beam is bent toward the direction of Super-K by  $80.7^\circ$ , with 104m radius of curvature, using 14 doublets of superconducting combined function magnets [4–6] (SCFMs). At intervals of SCFMs, three pairs of horizontal and vertical superconducting steering magnets are installed to correct the beam orbit. In the final focusing section, ten normal conducting magnets guide and focus the beam onto the production target, while directing the beam downward by  $3.637^\circ$ . The beam duct, inside of the primary beamline, is kept at high vacuum. A well-tuned proton beam is essential for the stable neutrino beam production, and to minimize beam loss in order to achieve high-power beam operation. Therefore, the intensity, position, profile and loss of the proton beam in the primary sections have been precisely monitored. This is achieved by five current transformers (CTs), 21 electrostatic monitors (ESMs), 19 segmented secondary emission monitors (SSEMs) and 50 beam loss monitors (BLMs). Their location is shown in Fig. 2.7.

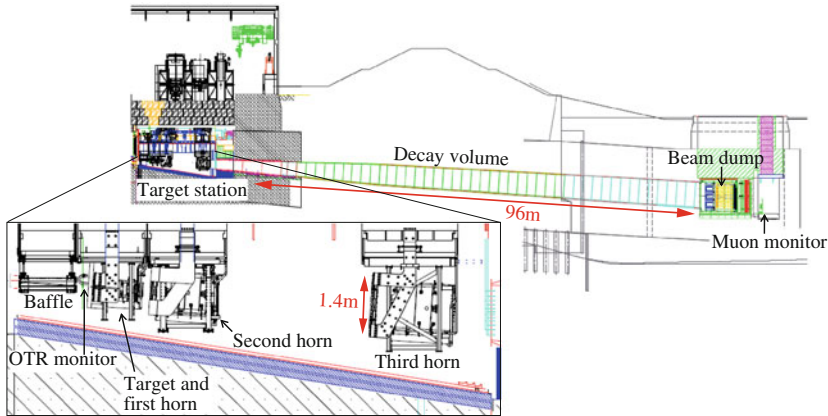


**Fig. 2.8** Side view of the secondary *beamline*

### 2.3.2 Secondary Beamline

The secondary beamline consists of four sections (Fig. 2.8): the target station, decay volume, beam dump and muon monitor.

#### 2.3.2.1 Target Station

The proton beam from the primary beamline goes through the baffle, which is a graphite block with a beam hole of 30 mm in a diameter, and impinges the production target. The optical transition radiation (OTR) monitor [7] is installed between the baffle and the target to monitor the beam profile and center. The target core is a 91.4 cm long, 2.6 cm diameter graphite [8] and is sealed inside a 0.3 mm thick titanium case as shown in Fig. 2.9. The target assembly is cantilevered inside the bore of the first horn inner conductor. In T2K, three magnetic horns are used. Each horn consists of two coaxial (inner and outer) conductors which encompass a closed volume [10, 11]. A toroidal magnetic field is generated in that volume. The field varies in inverse proportion to the distance from the horn axis. The first horn collects the charged pions that are produced at the target installed in its inner conductor as illustrated in Fig. 2.10. The second and third horns focus the pions. In the Run 1-4 operation, positive pions had been focused to produce neutrinos.<sup>3</sup> However, when the polarity of the horn current is inverted, negative pions are focused and antineutrinos are produced.

<sup>3</sup>Even when the positive pions are focused, antineutrinos mix in the neutrino beam by about 5 %.

**Fig. 2.9** Cross section view of the target

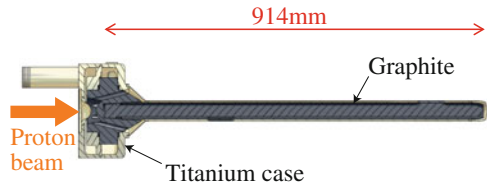
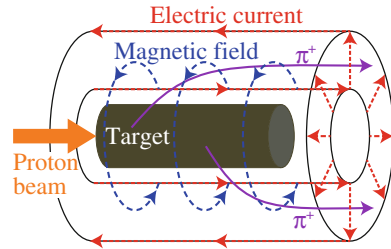


**Fig. 2.10** Illustration of the first horn



### 2.3.2.2 Decay Volume and Beam Dump

The pions decay to muon neutrinos and muons in the decay volume. The decay volume is a 96 m long steel tunnel. The cross section is 1.4 m wide and 1.7 m high at the entrance, and 3.0 m wide and 5.0 m high at the end. At the end of the decay volume, there is a beam dump composed of graphite blocks and concrete walls. The beam dump stops all the particles except for neutrinos and high energy muons.

### 2.3.2.3 Muon Monitor (MUMON)

The neutrino beam intensity and direction can be indirectly monitored on a bunch-by-bunch basis by measuring the profile distribution of muons after the beam dump. Since the muons are produced from the same parent particles as the neutrinos, the measurement of their properties also provides information about the neutrino beam indirectly. This is achieved by the muon monitor (MUMON) [12, 13] which is located behind the beam dump at a distance of 118 m from the production target, as shown in Fig. 2.8. It consists of two kinds of detector arrays: ionization chambers and silicon PIN photodiodes. Each array consists of  $7 \times 7$  sensors at 25 cm intervals and covers a  $150 \times 150 \text{ cm}^2$  area. The photograph of the muon monitor and the typical charge distribution of silicon arrays are shown in Fig. 2.11. The center of the muon profile can be measured with 2.95 cm accuracy, which corresponds to 0.25 mrad precision on the beam direction.

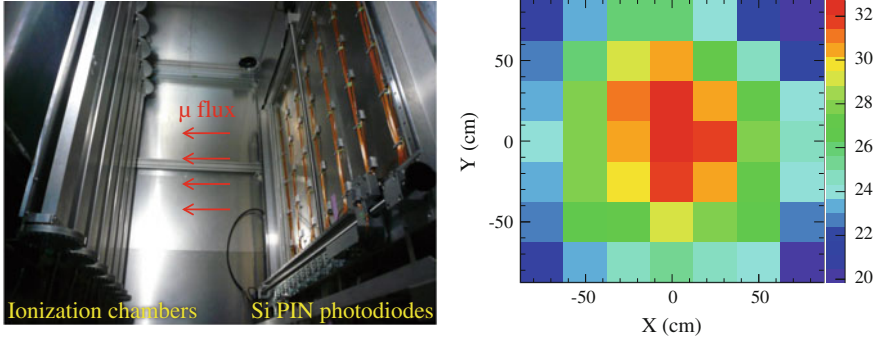


**Fig. 2.11** The photograph of the muon monitor (*left*) and the typical charge distribution of silicon arrays (*right*)

## 2.4 Near Detectors

The T2K near neutrino detectors are composed of the on-axis neutrino beam monitor (INGRID) and the off-axis neutrino spectrometer (ND280) as shown in Fig. 2.12. These detectors are housed in a pit inside the detector hall whose diameter and depth are 17.5 and 37m respectively that is located 280 m downstream from the production target.

**Fig. 2.12** The T2K near detectors (INGRID and ND280)

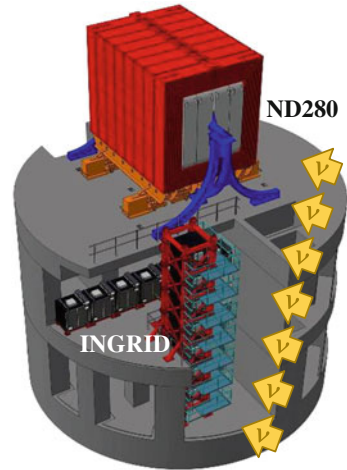
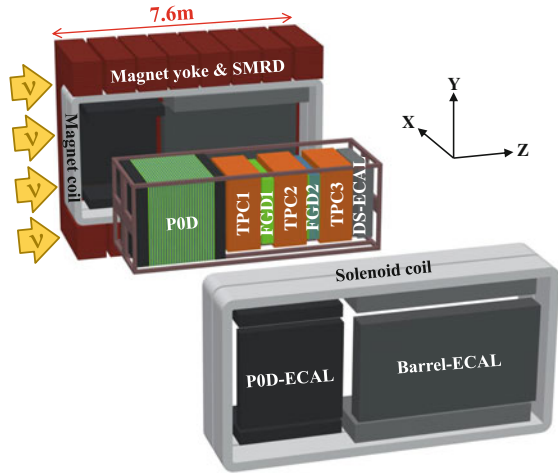




**Fig. 2.13** Exploded view of the ND280 detector



### 2.4.1 INGRID

INGRID (Interactive Neutrino GRID) [14] is a neutrino detector centered on the neutrino beam axis. Its main purpose is to measure the on-axis neutrino beam profile to monitor the neutrino beam direction. Details of INGRID are described in Chap. 3.

### 2.4.2 ND280

The ND280 detector is a complex of many components as shown in Fig. 2.13.

- A Pi-Zero Detector (P0D) [15] is placed at the upstream end to measure the neutral current  $\pi^0$  production rate for the estimation of the background against the  $\nu_\mu \rightarrow \nu_e$  signal at Super-K.
- Three Time Projection Chambers (TPC1,2,3) [16], together with two Fine Grained Detectors (FGD1,2) [17] are placed downstream of P0D to measure charged current interactions.
- An Electromagnetic Calorimeter (ECal) [18] surrounds P0D, TPCs, and FGDs.
- A magnet<sup>4</sup> provides a dipole magnetic field of 0.2T to measure momenta with good resolution and determine the sign of charged particles.
- A Side Muon Range Detector (SMRD) [21] is instrumented on all sides of the magnet.

<sup>4</sup>The magnet was used in the UA1 experiment [19] and the NOMAD experiment [20] at CERN and then was donated to T2K.

All the sub-detectors other than TPCs are based on extruded scintillators. ND280 is a totally different type of detector from Super-K because a large water Cherenkov detector in 280m location from the production target works poorly due to event pileup. In this thesis, FGDs and TPCs are used. FGDs consist of layers of finely segmented scintillating bars. They provide a target for neutrino interactions as well as tracking of charged particles coming from the neutrino interaction vertex. The outer dimensions and the total target mass of FGDs are  $2.3 \times 2.4 \times 3.65$  m (width, height, depth in beam direction) and 1.1 tons, respectively. TPCs use a gas mixture of  $\text{Ar}:\text{CF}_4:\text{C}_4\text{H}_{10}$  (95:3:2) and MicroMEGAS [22] readout planes. They measure the momentum of charged particles from the track curvature in a magnetic field as well as the amount of ionization left by each particle to identify the types of charged particles with combination of the measured momentum.

## 2.5 Super-Kamiokande Detector

### 2.5.1 Detector Overview

The world's largest land-based water Cherenkov detector, Super-Kamiokande (Super-K) [23], serves as the far detector in the T2K experiment. The detector is located 295 Km west of J-PARC, 1 km deep inside a mountain.<sup>5</sup> It is a cylindrical cavern, 39.3 m in diameter and 41.4 m in height, filled with 50 kton of pure water. It is optically separated by a cylindrical stainless steel structure to make two segments as shown in Fig. 2.14.

- The inner detector (ID) is a cylindrical shell of 33.8m in diameter and 36.2m in height. It houses 11,129 inward-facing 50cm diameter photomultiplier tubes (PMTs) along its inner walls, covering the 40 % of the surface.
- The outer detector (OD) is a 2 m-thick space enclosing the inner detector. It contains 1,885 outward-facing 20cm diameter PMTs along its inner walls. It is only sparsely instrumented with PMTs, but is capable of 100 % rejection efficiency of cosmic ray muon backgrounds.

The fiducial volume of Super-K is defined as a virtual cylinder of 29.8m in diameter and 32.2m in height ( $>2$  m from the ID wall), filled with 22.5 kton of pure water. Neutrinos are detected with the PMTs by measuring the Cherenkov lights emitted by charged particles from the neutrino interactions in the water. The particle's vertex, energies, directions are reconstructed from the timing and position of the Cherenkov lights. The particle identification (muon/electron separation) is performed based on the edge of the Cherenkov light pattern: the Cherenkov light pattern by a muon has a sharp edge, while that by an electron has a characteristic fuzzy edge due to electromagnetic showers.

---

<sup>5</sup>Cosmic muon rate in Super-K is 2Hz which is  $10^{-5}$  of that above ground.

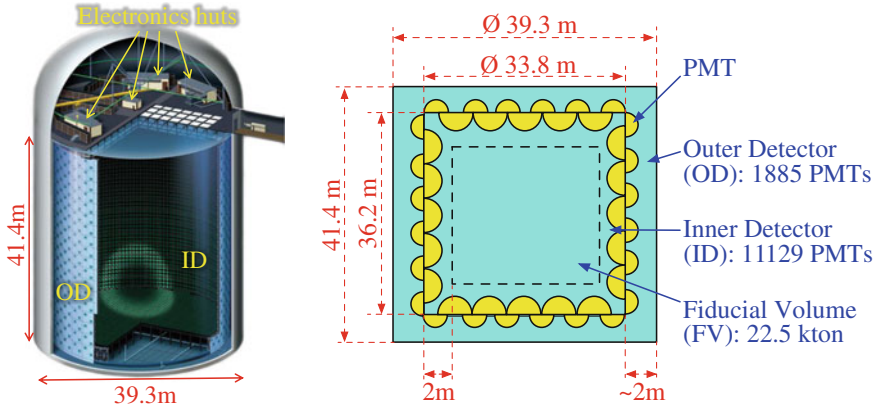


**Fig. 2.14** Schematic overview of Super-K (*left*) and cross section view of the Super-K water tank (*right*)

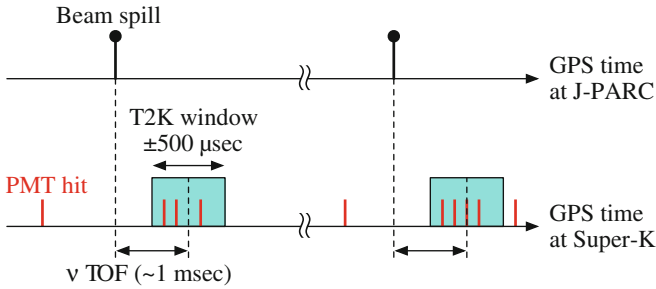


**Fig. 2.15** Overview of Super-K event timing

### 2.5.2 T2K Beam Data

The charge and timing of each hit PMT (hit threshold is  $\sim 0.25$  photoelectrons) are continuously collected, and are built as an event by an online software-trigger program. The T2K beam data is acquired by recording all hits within  $\pm 500 \mu\text{s}$  from the beam arrival time<sup>6</sup> (Fig. 2.15). The beam arrival time is determined by utilizing the GPS time synchronized between J-PARC and Super-K; the T2K beam neutrinos are expected to arrive at Super-K approximately 1 msec after the proton beam hits on the production target, where 1 msec is the neutrino TOF (Time of Flight) for 295 km. Further offline reduction of the T2K beam data is described in Chap. 10.

<sup>6</sup>Probability of observing accidental atmospheric neutrinos in five-year beam operation is less than 1 %.

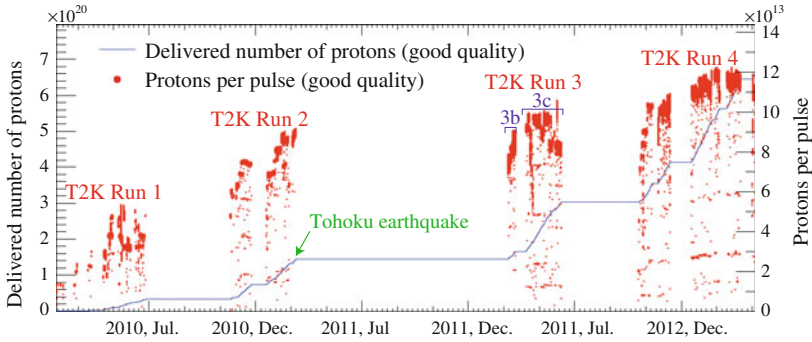


**Fig. 2.16** History of total accumulated protons and protons per pulse for the good quality beam data

**Table 2.2** Accumulated POT and horn current in each T2K data-taking period

Run period	Dates	Horn current (kA)	Accumulated POT
Run 1	Jan. 2010–Jun. 2010	250	$0.32 \times 10^{20}$
Run 2	Nov. 2010–Mar. 2011	250	$1.11 \times 10^{20}$
Run 3b	Mar. 2012	205	$0.22 \times 10^{20}$
Run 3c	Apr. 2012–Jun. 2012	250	$1.37 \times 10^{20}$
Run 4	Oct. 2012–May. 2013	250	$3.56 \times 10^{20}$
Total	Jan. 2010–May. 2013		$6.57 \times 10^{20}$

## 2.6 Data Set

The physics results presented in this thesis are based on four physics runs: Run 1 (January – June 2010), Run 2 (November 2010 – March 2011), Run 3 (March – June 2012) and Run 4 (October 2012 – May 2013). The Run 3 period is divided into three sub periods, Run 3a (March 2012), Run 3b (March 2012) and Run 3c (April – June 2012), according to the horn current settings (with a 0 kA setting in Run 3a and a 205 kA setting in Run 3b instead of the nominal 250 kA).<sup>7</sup> The Run 3a data is not used for the oscillation analysis because the data in this period is small (0.1 % of the total) and the horn current was set to 0 kA. We select only good quality beam data for physics analysis using the following conditions.

- Each hardware component works normally.
- The deviation of all horns currents from the mean is within  $\pm 5$  kA.
- The deviation of the beam angle measured by MUMON from the mean is within 1 mrad.

<sup>7</sup>Since the power supply of the horns were broken just before Run 3, Run 3 was started without operating horns. Then the horn operation was started with lower current settings.

- The deviation of the total muon yield measured by MUMON from the mean is within  $\pm 5\%$ .

After the good quality cut, the fraction of beam data remained is 99.8 %. Figure 2.16 shows the accumulated protons on target (POT) and protons per pulse for good quality beam data over time, and Table 2.2 summarizes the accumulated POT and horn current in each run period. The total accumulated POT in all run periods is  $6.57 \times 10^{20}$  POT, corresponding to 8 % of T2K's exposure goal. The maximum proton beam power reached so far is 235 kW.

## References

1. D. Beavis, A. Carroll, I. Chiang et al., Physics Design Report, BNL 52459 (1995)
2. D. Ayres et al., (NO $\nu$ A Collaboration), Fermilab-Proposal-0929 (2005)
3. Y. Yamazaki et al., KEK-Report 2002-13; JAERI-Tech 2003-044 (2003)
4. T. Nakamoto et al., IEEE Trans. on Appl. Superconductivity **14**, 616 (2004)
5. T. Nakamoto et al., Proceedings of 2005 Particle Accelerator Conference (2005)
6. T. Ogitsu et al., IEEE Trans. on Appl. Superconductivity **15**, 1175 (2005)
7. S. Bhadra et al., Nucl. Instrum. Meth. A **703**, 45 (2013)
8. T. Nakadaira et al., AIP Conf. Proc. **981**, 290 (2008)
9. A.K. Ichikawa, Nucl. Instrum. Meth. A **690**, 27 (2012)
10. S. van der Meer, CERN-61-07 (1961)
11. R. Palmer, CERN-65-32 (1965)
12. K. Matsuoka et al., Nucl. Instrum. Meth. A **623**, 385 (2010)
13. K. Matsuoka et al., Nucl. Instrum. Meth. A **624**, 591 (2010)
14. K. Abe et al., T2K Collaboration. Nucl. Instrum. Meth. A **694**, 211 (2012)
15. S. Assylbekov et al., Nucl. Instrum. Meth. A **686**, 48 (2012)
16. N. Abgrall et al., Nucl. Instrum. Meth. A **637**, 25 (2011)
17. P.A. Amaudruz et al., Nucl. Instrum. Meth. A **696**, 1 (2012)
18. D. Allan et al., J. Instrum. **8**, 10019 (2013)
19. M.B. Luque et al., UA1 Collaboration. Nucl. Instrum. and Meth. **176**, 175 (1980)
20. J. Altegoer et al., NOMAD Collaboration. Nucl. Instrum. Meth. A **404**, 96 (1998)
21. S. Aoki et al., Nucl. Instrum. Meth. A **698**, 135 (2013)
22. I. Giomataris et al., Nucl. Instrum. Meth. A **560**, 405 (2006)
23. Y. Fukuda et al., Super-Kamiokande Collaboration. Nucl. Instrum. Meth. A **501**, 418 (2003)

<http://www.springer.com/978-981-287-714-7>

Measurement of Neutrino Interactions and Three Flavor  
Neutrino Oscillations in the T2K Experiment

Kikawa, T.

2016, XX, 264 p., Hardcover

ISBN: 978-981-287-714-7